Icarus 273 (2016) 205–213

Contents lists available at ScienceDirect

Icarus

journal homepage: www.elsevier.com/locate/icarus

The temperatures of Giordano Bruno crater observed by the Diviner Lunar Radiometer Experiment: Application of an effective field of view model for a point-based data set

J.-P. Williams[a,*], E. Sefton-Nash[b], D.A. Paige[a,1]

[a] Dept. Earth, Planetary and Space Sciences, University of California, Los Angeles, CA 90095, USA
[b] Department of Earth and Planetary Sciences, Birkbeck, University of London, Malet Street, London WC1E 7HX, UK

ARTICLE INFO

Article history:
Received 29 June 2015
Revised 30 September 2015
Accepted 29 October 2015
Available online 14 November 2015

Keywords:
Moon
Moon, surface
Regoliths
Cratering
Infrared observations

ABSTRACT

Point based planetary datasets are typically stored as discrete records that represent an infinitesimal location on the target body. Instrumental effects and spacecraft motion during integration time can cause single points to inadequately represent the total area on the target that contributes to an observation. Production of mapped data products from these data for scientific analysis proceeds by binning points onto rectangular grids. Empty bins occur where data coverage is insufficient relative to grid resolution, a common problem at high latitudes in cylindrical projections, and remedial interpolation can lead to high uncertainty areas and artifacts in maps.

To address such issues and make better use of available data, we present a method to calculate the ground-projected effective field of view (EFOV) for point-based datasets, using knowledge of instrumental characteristics and observation geometry. We apply this approach to data from the Lunar Reconnaissance Orbiter (LRO) Diviner Lunar Radiometer Experiment, a visible to far-infrared multispectral radiometer which acquires radiometric measurements of reflected visible and emitted infrared radiation of the Moon in 9 spectral channels between 0.35 and 400 μm. Analysis of gridded radiance from crater Giordano Bruno, a 22 km diameter rayed crater, is used to demonstrate our gridding procedure. Diviner data, with such processing, reveals details of the surface that are seen in the high-resolution LRO Camera NAC images. Brightness temperatures and anisothermality observed in Diviner's IR channels show the thermophysical properties of the crater ejecta to be very heterogeneous indicative of minimal mechanical disruption by micrometeoroid impacts consistent with a very young (<10 Ma) formation age as the lunar surface becomes rapidly homogenized over time. This heterogeneity has implications for crater-count studies as regions of high anisothermality are characterized by large blocks of material and lower crater densities.

1. Introduction

The Diviner Lunar Radiometer Experiment (Paige et al., 2010a) is one of seven instruments aboard NASA's Lunar Reconnaissance Orbiter (LRO) (Chin et al., 2007; Tooley et al., 2010; Vondrak et al., 2010). Diviner began operating July 5, 2009, mapping the Moon on a nearly continuous basis, acquiring calibrated radiometric measurements of reflected visible, and emitted infrared radiation of the Moon in 9 spectral channels covering a wavelength range of 0.3–400 μm. Each Diviner channel is comprised of a 21-element thermopile detector array and spectral filter. The instrument nominally points in the nadir direction operating as a multi-spectral pushbroom mapper. Observations are acquired continuously with a 0.128 s signal integration period, providing a swath width of 3.4 km and a nominal instantaneous field of view (IFOV) of 320 m in-track and 160 m cross-track for each detector at an orbital altitude of 50 km.

The Diviner Commissioning and Primary Mapping dataset, covering July 5, 2009 to September 15, 2012, have been gridded into global brightness temperature maps referred to as Diviner Global Data Records (GDR), which have been archived at the NASA Planetary Geosciences Node (LRO-L-DLRE-5-GDR-V1.0) (Paige et al., 2011). These gridded data products were derived directly from the Reduced Data Records (RDR) products: level 1 calibrated radiance observations (Sullivan et al., 2013). Diviner GDR data products are

* Corresponding author. Fax: +1 310 825 2279.
E-mail addresses: jpierre@mars.ucla.edu (J.-P. Williams), e.sefton-nash@uclmail.net (E. Sefton-Nash), dap@moon.ucla.edu (D.A. Paige).
[1] Fax: +1 310 825 2279.

http://dx.doi.org/10.1016/j.icarus.2015.10.034
0019-1035/

not interpolated and include data gaps in grid cells where no observations were acquired.

The data gridding approach described in this paper was developed and used for the creation of all archived Diviner GDR products (Paige et al., 2011) and is routinely employed when gridding Diviner data. We therefore use Diviner as an example to illustrate our approach, though our procedure in this paper is not necessarily Diviner specific. We then present analysis of Diviner data from two orbits tracks crossing the crater Giordano Bruno showing how the thermal response of the surface material within and around the crater to solar forcing reveals a complex, and heterogeneous mixture of thermophysical properties, consistent with a very young crater that has experienced minimal processing by micrometeoroid bombardment.

2. Calculating the effective field-of-view (EFOV)

For an instrument operating in a pushbroom configuration like Diviner, the effective FOV in the in-track direction is broadened by two effects: (i) spacecraft motion relative to the target body during the sample integration time $b(t)$ and (ii) the exponential detector thermal response time $d(t)$. These effects result in elongation of the FOV in the in-track direction, and along with the instrument's instantaneous field of view (IFOV) $f(t)$, define the total contribution to an observation. Knowing the shape of these functions, for each observation we may construct a 2D probability distribution in the focal plane of the detector – equal to a convolution of the component functions evaluated over the integration time: $[(b * d) * f](t)$. This EFOV describes the likelihood of quanta e.g., photons, originating from a given location within an observation's ground projected footprint.

In order to produce mapped data products, the probability function must be discretized into points so that they may be projected onto the surface of the target body (assuming there is knowledge of the observation geometry), and subsequently binned onto regular grids. This is accomplished by populating the EFOV with a Monte Carlo distribution comprising n points, where the weight of each point $w = 1/n$ observations. The term n must be sufficient to adequately resolve the EFOV with the modeled EFOV tending to the actual EFOV with increasing n.

The instantaneous field of view for each Diviner detector was measured in the laboratory prior to integration with LRO (see Paige et al. (2010a) for details). The average IFOV of all 21 detectors for each channel are shown in Fig. 1 with measured step sizes of 0.39 mrad and 0.19 mrad for in-track and cross-track scans, respectively. Shoulders with a magnitude ~5–10% of the central peak in the cross-track IFOVs are due to thermal crosstalk between adjacent detectors. Channels 2 and 6 are narrow in the in-track IFOVs due to reduced apertures over these spectral filters. The three longest wavelength channels (7–9) have the broadest fields of view due to the mesh filters employed for these channels (Paige et al., 2010a).

Each detector has a thermal response time associated with it (i.e. each detector has a memory of an observation that decays exponentially with time). Table 1 shows the response time, $t_\circ$, for the individual Diviner channels. The exponential function representing the detector response time is $\exp(\alpha/x_\circ)$, where α is the angular distance in radians from the center of the observation (assumed to be nadir pointing in this discussion) and $x_\circ = \tan^{-1}(v_{sc}t_\circ/z_{sc})$ is a decay constant related to the detector response time, the spacecraft velocity v_{sc}, and altitude z_{sc} at the mid-point of the observation. Spacecraft motion during the 128 ms sample integration time results in additional smearing in the in-track direction represented by a triangular function (Fig. 2). The effective in-track FOV is then the convolution of the triangular function with the in-track IFOV and the exponential function representing the detector response

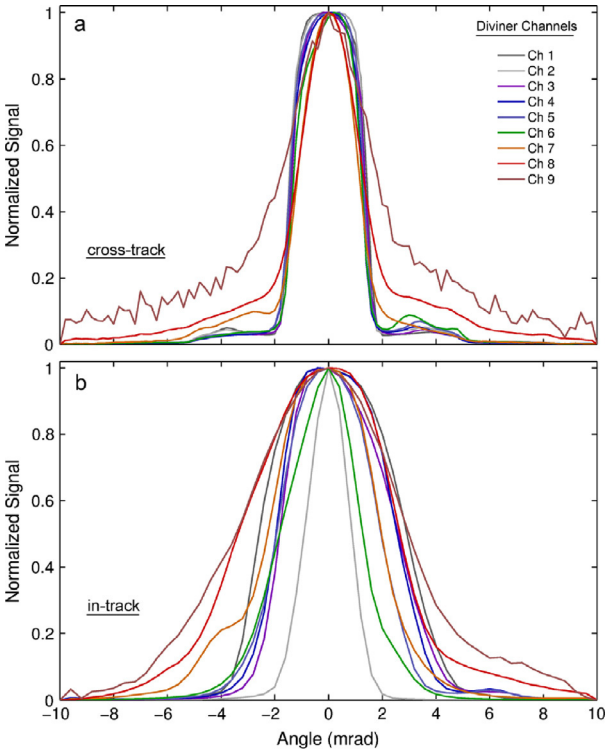

Fig. 1. (a) Cross-track and (b) in-track instantaneous fields of view of Diviner channels.

Table 1
Diviner exponential detector thermal response times.

Channel	Passband (μm)	Response time, $t_\circ$ (ms)
1	0.35–2.8	110
2	0.35–2.8	110
3	7.55–8.05	119
4	8.10–8.40	123
5	8.38–8.68	123
6	13–23	117
7	25–41	127
8	50–100	131
9	100–400	147

time. Fig. 2 shows the Diviner channel 4 IFOVs, the two functions representing integration time and detector response time broadening, and the EFOV resulting from the convolution of the other three functions assuming the LRO nominal mapping orbit configuration: near-circular orbit at an altitude ~50 km with a ground speed ~1.66 km s^{-1}. All functions are normalized to a value of one. No broadening occurs in the cross-track direction. The resulting two-dimensional EFOV is ellipsoidal with elongation in the in-track direction. The resulting shape of the EFOV will depend on altitude and ground speed and therefore will differ with changing orbital parameters.

3. Gridding data

In determining the effective surface footprint of the detectors, the orientation of the detectors must first be determined. Fig. 3 shows the basic viewing geometry of the array of Diviner detectors. To determine their orientation relative to north, we define a plane determined by the vector from the center of the Moon to the latitude and longitude of the point observation on the surface, **s**, and the vector defining the lunar spin axis in the north direction **N**. The orientation of the detectors is defined by a vector **d**, aligned with the detector array and projected from the lunar center to the